

EFFECT OF PARTICLE SIZE ON THE FRACTURE BEHAVIOUR  
OF ALUMINIUM HYDROXIDE FILLED POLYPROPYLENE

J.I. Velasco\*, C. Morhain†, M.Ll. Maspocho\* and O.O. Santana†

The effect of filler particle size on the fracture behaviour of PP/Al(OH)<sub>3</sub> composites was investigated at a concentration level of 20 vol/vol % of filler. Two grades of Al(OH)<sub>3</sub> having different average particle sizes (1.5 and 60 µm) were used as fillers in a polypropylene homopolymer, and the fracture characterization of the composites was based on LEFM analysis from impact data, which were obtained using an instrumented Charpy impact pendulum on injection-moulded SENB specimens with a large range of initial crack lengths. It was shown that under the conditions applied the LEFM analysis seems to be valid to characterize the fracture toughness of these materials. The composite filled with the finest grade of Al(OH)<sub>3</sub> showed higher stiffness, tensile strength, fracture toughness and fracture energy than the composite filled with coarser particles.

INTRODUCTION

Aluminium hydroxide is a flame retardant filler traditionally used in thermoset polymers; its use in thermoplastics is fairly recent as a consequence of the efforts made to eliminate the halogen-based flame retardant additives from the plastic formulations. Unfortunately, high contents of Al(OH)<sub>3</sub> are usually required for a good flame retardancy, which can promote important modifications in the mechanical behaviour of thermoplastics like polypropylene (Liauw et al (1)); other factors like particle size and shape, and the particle surface treatment (1) can also affect strongly the mechanical behaviour and the fracture of these particulate filled polymers. To promote linear-elastic behaviour and brittle fracture in PP composites high-rate fracture tests must be performed using impact devices. Moreover, to have instrumented impact data with negligible dynamic effects, the impact tests must be carried out with a high effective mass and at a moderate impact rate. The aim of this paper is to present an instrumented Charpy impact application to the fracture characterization of injection-moulded PP/Al(OH)<sub>3</sub> composites, through the influence of the Al(OH)<sub>3</sub> particle size. Here, the fracture parameters  $K_{IC}$  and  $G_{IC}$  were obtained applying the LEFM analysis to the impact data and, previously, a low-rate tensile characterization was carried out to determine the Young's modulus and the yield strength of the composites.

\* Department of Materials Science, Universitat Politècnica de Catalunya, Barcelona, Spain

† Centre Català del Plàstic, Terrassa, Spain.

## EXPERIMENTAL

Materials, compounding and specimens

Two commercial grades (*Martinal* ON and OL-104-LE) of uncoated  $\text{Al}(\text{OH})_3$  were employed as fillers into a PP homopolymer matrix (*Isplen* PP050). The ON filler had irregular, approximately spherical particles with a mean diameter of 60  $\mu\text{m}$  and a specific surface area of 0.5  $\text{m}^2/\text{g}$ , whereas the OL grade had a mean particle diameter of 1.5  $\mu\text{m}$  and a specific surface area of 3.1  $\text{m}^2/\text{g}$ . The OL grade notwithstanding had a small fraction of hexagonal plates. With 40 wt.% of both grades of  $\text{Al}(\text{OH})_3$  two composites, named PPOL and PPON respectively, were prepared using a co-rotating twin screw extruder (screw diameter 25 mm and  $L/D = 24$ ). The cylinder temperature profile was 160, 180, 185, 190, 195  $^{\circ}\text{C}$  and the speed 80 rpm. The unfilled PP was also extruded to have in it the same thermal and mechanical histories than in the filled samples. The respective extrudates were cooled in water and pelletised. Table 1 shows the initial characteristics of the samples.

Standard tensile specimens (type "I" according to ASTM D638) and prismatic bars with overall dimensions  $B \times W \times L = 6.35 \times 12.7 \times 127 \text{ mm}^3$  were injection-moulded using a 90/440 injection moulding machine. The melt temperature was 200  $^{\circ}\text{C}$  and the nominal injection pressure 100 MPa. For fracture tests single-edge notched three point bend (SENB) specimens with overall dimensions  $6.35 \times 12.7 \times 63.5 \text{ mm}^3$  were prepared by cutting the injected bars into halves. Notches were machined centrally on the narrowest side using a 45 $^{\circ}$  "V" notch broaching tool with a tip radius of 0.25 mm, and sharpened with a single cut ( $\approx 0.2 \text{ mm}$  deep) from a razor blade having a tip radius of about 1-2  $\mu\text{m}$ . Cracks of various initial lengths ( $a_0$ ) were inserted using this technique.

Testing procedure

Tensile tests were carried out with an universal testing machine and an optical extensometer. The Young's modulus was obtained from the slope of the initial region of the strain/stress curve, and the maximum stress was taken as the material yield strength. To analyse the influence of the strain rate on the mechanical characteristics, tensile tests were realized at four different cross-head speeds (5, 10, 50, 100 mm/min). Moreover, the yield strength values obtained from these low-rate tests were extrapolated, on a logarithmic time-scale, to have high-rate yield strength values useful for the fracture analysis.

TABLE 1- Initial characteristics of the samples. MFI measured at 190  $^{\circ}\text{C}$  and 2.16 kg, and HDT measured at 120  $^{\circ}\text{C}/\text{h}$  and 1.8 MPa.

Sample	$\text{Al}(\text{OH})_3$ Concentration (% by weight)	$\text{Al}(\text{OH})_3$ Concentration (% by volume)	Density ( $\text{g}/\text{cm}^3$ )	MFI ( $\text{g}/10 \text{ min}$ )	HDT ( $^{\circ}\text{C}$ )
PP	0	0	0.922	2.19	70
PPOL	39.8	19.7	1.184	1.50	116
PPON	39.6	19.3	1.160	1.66	114

Three-point bend fracture tests were carried out on the above described SENB specimens using a instrumented Charpy impact pendulum. The span ( $S$ ) was 50.8 mm, the effective mass of the hammer 2.508 kg and the initial speed 0.973 m/s. Three different load/time curves were recorded for each specimen, which correspond to the respective load transducers mounted on the striker and on both supports. At least 12 specimens, having different initial crack lengths in the range 1-7 mm, were tested for each material. Unnotched specimens were also used to determine the modulus of elasticity by rebound at the same conditions than the fracture tests. All the experiments were done at room temperature. The fractures surfaces were observed by scanning electron microscopy (SEM), after the samples were gold-coated.

## RESULTS AND DISCUSSION

### Tensile behaviour

As expected, the presence of rigid  $\text{Al(OH)}_3$  particles in the PP matrix increased the material stiffness, reduced the yield strength due to a weak particle/matrix interface that early promoted debonding, and also reduced the material elongation because the particles limited the matrix flow (see the MFI and HDT values in Table 1). Due to the approximately spherical shape of the  $\text{Al(OH)}_3$  particles, the obtained values of the composites Young's modulus (Fig. 1) were between the values predicted by the Kerner-Nielsen equation (Nilesen (2)), using  $v_m = 0.42$  and  $E_p = 75$  GPa (1)

$$E_c = E_m \frac{1 + ABV_p}{1 - BV_p} \quad \text{with} \quad A = \frac{7 - 5v_m}{8 - 10v_m} \quad B = \frac{E_p/E_m - 1}{E_p/E_m + A} \quad (1)$$

and those predicted by the Tsai approximation for randomly oriented particles (2)

$$E_c = \frac{3}{8} E_{\parallel} + \frac{5}{8} E_{\perp} \quad (2)$$

For theoretical analysis of  $E_{\perp}$  we used the Kerner-Nielsen equation, and for  $E_{\parallel}$  the equation proposed by Halpin (3) for unidirectionally oriented short fibres, with  $A = 5$

$$E_c = E_m \frac{1 + ABV_p}{1 - BV_p} \quad A = l/r \quad (3)$$

The values of the PPOL Young's modulus were found to be slightly higher than those of the PPON. Considering there are more interfacial interactions in the composite filled with particles of higher specific surface area (PPOL), the extent of immobilized, more rigid PP around the particles in this sample could be greater than in the PPON, contributing to increase the Young's modulus. The presence of a fraction of anisometric, platy  $\text{Al(OH)}_3$  particles in the PPOL sample could also contribute to the higher  $E_c$  observed values due to particle orientation effects during the specimens injection-moulding.

The obtained yield strength values have also been compared with those predicted by two different models. Since the Al(OH)<sub>3</sub> particles used in this work were not surface-treated to improve its adhesion with PP, we have applied the simplest theoretical model derived for composites filled with short fibres of length lesser than the critical value, assuming that the interfacial shear strength is zero, and also the Nicolais-Narkis equation. These equations have been reviewed by Danusso and Tieghi (4).

$$\sigma_{yc} = \sigma_{ym} (1 - V_p) \quad (4)$$

$$\sigma_{yc} = \sigma_{ym} (1 - 1.21 V_p^{2/3}) \quad (5)$$

As shown in Fig. 2, the values of the PPOL yield strength matched well with the simplest theoretical model, that is to say just the area of matrix normal to the stress direction contributed to the composite strength; whereas the PPON yield strength was found to be lower. The possible cause of this reduction could be a worse wetting of the coarser particles, which would give rise to a larger fraction of voids in the composite. Owing to the viscoelastic behaviour of polypropylene, both yield strength and Young's modulus increased as the strain rate was raised.

#### Fracture behaviour

The three studied materials showed unstable fracture behaviour with the conditions imposed on the impact tests, and the fracture toughness was evaluated by a LEFM analysis. As shown in Fig. 3, the fracture toughness ( $K_{IC}$ ) and the fracture energy ( $G_{IC}$ ) were achieved from the  $F_{max} S / BW^{3/2}$  versus  $1/f$  and from  $U_{peak}$  versus  $BW\phi$  plots, respectively.  $F_{max}$  and  $U_{peak}$  were the average values of those obtained from the three load transducers of the pendulum. The results are shown in Table 2. Here  $E^{reb}$  represents the modulus of elasticity calculated from rebound tests as  $(F/d)(S/4BW^3)$ , where  $(F/d)$  was the slope of the initial linear region of the rebound load/displacement curve.

TABLE 2- Values of the LEFM parameters, elastic modulus, and yield strength at impact velocity.

Sample	$K_{IC}$ (MPa m <sup>1/2</sup> )	$G_{IC}$ (kJ/m <sup>2</sup> )	$E^{th} = K_{IC}^2(1-\nu^2)/G_{IC}$ (GPa)	$E^{reb}$ (GPa)	$\sigma_y$ (MPa)	$2.5 K_{IC}^2/\sigma_y^2$ (mm)
PP	2.36	2.40	1.92	2.09	44.1	7.1
PPOL	2.43	2.07	2.44	2.51	35.6	11.6
PPON	2.22	1.82	2.32	2.33	32.8	11.4

No significant differences were found between the  $K_{IC}$  value of unfilled PP and those of the filled samples. Nevertheless, the fracture energy of the composites was clearly lower than that of the pure PP because of the filled samples higher stiffness. Such reduction was more significant for the PPOL sample. The PPON composite showed lower  $K_{IC}$  and  $G_{IC}$  values than the PPOL, and this effect could be justified if we consider the Al(OH)<sub>3</sub>

## ECF 12 - FRACTURE FROM DEFECTS

particles as inner defects of the material (Fig. 4); the bigger particle mean size the more important the defects are, which act as crack propagation starters, reducing the fracture toughness.

Although the specimen size criterion for plane strain conditions was not satisfied, the  $E^{reb}$  values matched quite well with the values of the elasticity modulus ( $E^{th}$ ) obtained from  $K_{IC}$  and  $G_{IC}$  using the theoretical expression for plane strain (Williams (5)). Therefore, our values could be taken as close to the material fracture parameters.

### CONCLUSIONS

It was shown that employing an instrumented impact pendulum an accurate selection of the test conditions allows us to apply the LEFM analysis to obtain fracture parameters of PP/Al(OH)<sub>3</sub> composites. The composite filled with the finest grade of Al(OH)<sub>3</sub> showed higher stiffness, tensile yield strength, fracture toughness and fracture energy than the composite filled with coarser particles.

### SYMBOLS USED

$E_c, E_m, E_p$	= Young's modulus of the composite, matrix and particle (GPa)
$E_{\parallel}, E_{\perp}$	= Young' modulus parallel and perpendicular to the filler direction (GPa)
$E^{reb}$	= elastic modulus from rebound test (GPa)
$F_{max}$	= maximum force in impact curves (N)
$f$	= calibration factor
$G_{IC}$	= critical strain energy release rate (kJ/m <sup>2</sup> )
HDT	= heat deflection temperature (°C)
$K_{IC}$	= critical stress intensity factor (MPam <sup>1/2</sup> )
MFI	= melt flow index (g/10 min)
$U_{peak}$	= energy stored up to the maximum force in impact tests (J)
$V_p$	= particle volume fraction
$\phi$	= energy calibration factor
$\nu$	= Poisson's ratio
$\sigma_{ic}, \sigma_{ym}$	= tensile yield strength of the composite and matrix (MPa)

### REFERENCES

- (1) Liauw, C.H., Lees, G.C., Hurst, S.J., Rother, R.N. and Dobson, D.C., *Plast. Rubb. Process. Appln.*, Vol. 24, 1995, pp. 249-260.
- (2) Nielsen, L.E., "Mechanical Properties of Polymers and Composites", Vol. 2, Marcel Dekker, New York, USA, 1972.
- (3) Halpin, J.C., *J. Comp. Mater*, Vol. 3, 1969, pp. 732-734.
- (4) Danusso, F. and Tieghi, G., *Polymer*, Vol. 27, 1986, 1385-1391.
- (5) Williams, J.G., "Fracture Mechanics of Polymers", E. Horwood, Chichester, UK, 1984

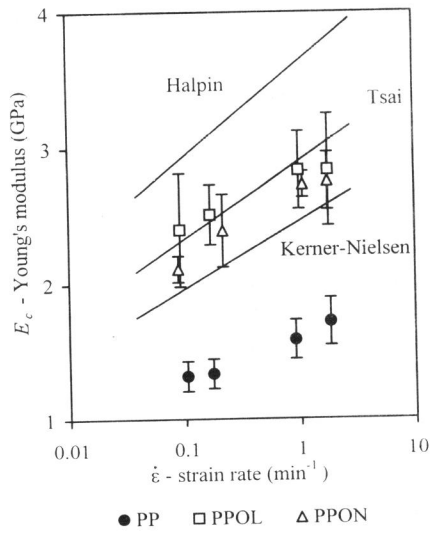


Figure 1. Measured Young's modulus and applied models.

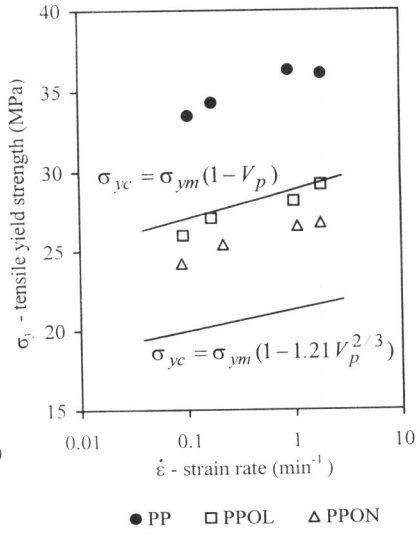


Figure 2. Measured tensile strength and applied models.

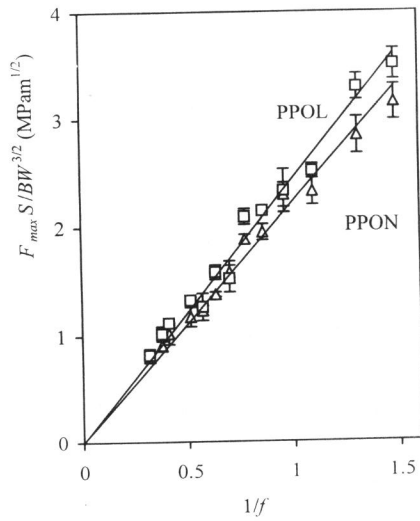


Figure 3. Graphical determination of  $K_{IC}$ .

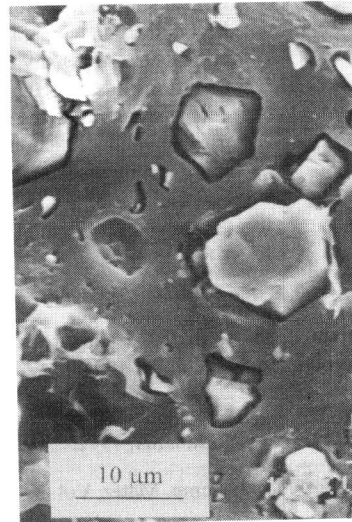


Figure 4. PPON fracture surface by SEM.